ISSN 1996-3394

# Asian Journal of Materials Science

http://knowledgiascientific.com

Knowledgia SCIENTIFIC
A Place to Publish Outstanding Research

Asian Journal of Materials Science 4 (2): 34-44, 2012
ISSN 1996-3394 / DOI: 10.3923/ajmskr.2012.34.44


# Mixed Mode Crack Initiation and Growth in Notched Semi-circular Specimens: Three Dimensional Finite Element Analysis

[1]H.E.M. Sallam and [2,3]A.A. Abd-Elhady

[1]Department of Civil Engineering, Jazan University, Jazan 706, Kingdom of Saudi Arabia; on Sabbatical Leave from Department of Materials Engineering, Zagazig University, Zagazig, 44519, Egypt
[2]Department of Mechanical Engineering, Jazan University, Jazan 706, Kingdom of Saudi Arabia
[3]Department of Mechanical Design, Faculty of Engineering, Helwan University, Cairo, Egypt

*Corresponding Author: H.E.M. Sallam, Department of Civil Engineering, Jazan University, Jazan 706, Kingdom of Saudi Arabia*

## ABSTRACT

A Semi-circular Bend (SCB) specimen containing an inclined U-shape edge notch was used to study mixed mode crack initiation and growth behavior in three-dimension. The effect of the inclination angle of the notch on the crack trajectory was studied. After identifying the crack path, mode I and II stress intensity factors for four different crack lengths on the real path were determined. The variations of mode I and II stress intensity factors on the crack front were also depicted. It is found for different inclination notch angle that, the crack initiated from the notch in SCB specimen at the point of the longest vertical coordinate on the notch surface. The maximum value of mode I normalized stress intensity factor occurs only on the mid plane in the case of pure mode I. However, this location moves away from the mid plane to the surface of the specimen by increasing the value of the mode mixity.

**Key words:** Mixed mode I/II, crack initiation angle, crack growth path, SCB specimen

## INTRODUCTION

Mode I fracture toughness, $K_{IC}$ or $G_{IC}$, of many advanced engineering materials such as bimaterial (Shah *et al*., 2005a, b), interlaminar mode I fracture toughness (Beng *et al*., 2007; Zenasni *et al*., 2006; Zulkifli *et al*., 2008), has received adequate attention from researchers. In practice the pre-existing cracks in the structures are often subjected to complex loading. For such cases, due to arbitrary orientation of flaws relative to the overall applied loads, cracks experience a combination of two major modes of loading: mode I and II (mixed mode I/II). The prediction of cracking direction and subsequent crack path is well-recognized problem. Recently, considerable research efforts have been to investigate crack growth behavior under mixed mode I/II loading. A variety of mechanics-based theories have been proposed and used by investigators to predict the direction of crack growth under mixed mode I/II loading (Hammouda *et al*., 2004; Muthurajan *et al*., 2006; Ouinas *et al*., 2006; Ravichandaran and Thanigaiyarasu, 2011; Shariati and Maghrebi, 2009). Under mixed mode loading conditions, fracture of cracked components and structures may grow along curvilinear paths and not necessarily along the direction of original crack. Aliha *et al*. (2010) studied the mixed mode I/II crack growth behavior

of guiting limestone by using a Semi-circular Bend (SCB) specimen. They observed that, trajectories crack is not only depending on the mode mixity but also on the specimen shape. Ayatollahi and Aliha (2007) presented the results of mixed mode fracture tests on PMMA in the full range from pure mode I to pure mode II obtained from the cracked SCB specimen. All of them deduced the same general formula for mode I normalized stress intensity factor $Y_I$ which is defined as:

$$Y_I = \frac{K_I}{\sigma_{ap}\sqrt{l\pi}} \quad (1)$$

And for mode II:

$$Y_{II} = \frac{K_{II}}{\sigma_{ap}\sqrt{l\pi}} \quad (2)$$

Where:
$K_I$ = Mode I stress intensity factor
$K_{II}$ = Mode II stress intensity factor:
$\sigma_{ap}$ = P/2Rt
t = Specimen thickness
P = Applied load
R = Radius of specimen
l = Crack length

The objective of this study was to analyze the mixed mode fracture behavior in three dimensions using SCB specimen. The effect of inclination angle of edge U-notch on the crack initiation and growth behavior was analyzed. The variation of mode I and II stress intensity factor through the crack thickness are described. It is worth to note that, all of the previous work did not determine the SIF of the stationary after its growth, i.e., ignore the real path of the propagating crack (Ayatollahi and Aliha, 2008). In the present analysis, the SIF was calculated for four different crack lengths on the real path of the crack growth for the different inclination angle of the notch.

## NUMERICAL WORK

SCB specimen of radius (R) containing an edge narrow U-notch of depth (D) and radius ($\rho$) was selected for this study, as shown in Fig. 1. The narrow notch makes an angle, $\beta$, relative to the vertical direction. The specimen is placed on two bottom supports of distance 2S and is loaded by the vertical displacement equal 1 mm. In the present study, the specimen radius and thickness (2B) are 50 and 5 mm, respectively. The values of D/R, S/R and D/$\rho$ are 0.3, 0.4 and 100, respectively. Four different notch inclination angles, $\beta$ = 0°, 10°, 20° and 30°, were considered. The angle to obtain pure mode II for the SCB specimen varies typically between 35 and 60° (Ayatollahi *et al*., 2006).

After prediction the crack path for different notch inclination angles, mode I and II SIF of crack emanating from that notch in real path, with crack length a equals 0.5, 1, 1.5 and 2 mm, were

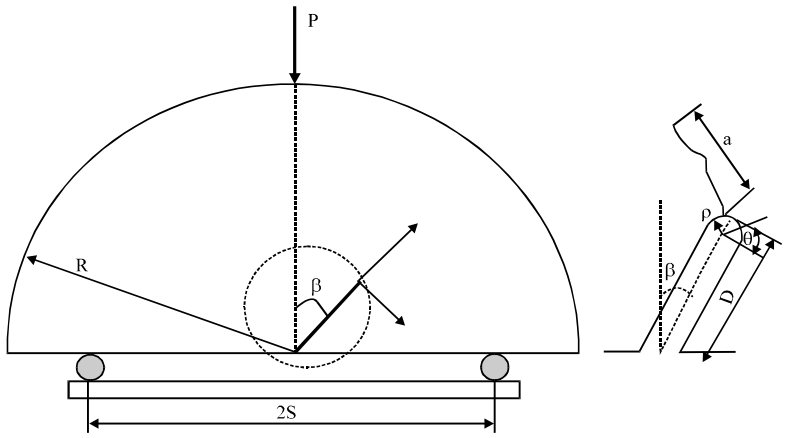


Fig. 1: Notched semi-circular bend (SCB) specimen

predicted. In the present finite element analysis, FE, the mechanical behavior of the SCB specimen material was assumed to be isotropic behavior.

**Finite element analysis:** Extend Finite Element Method (X-FEM) was used for simulating the fracture crack path (ABAQUS, 2002) in various crack analysis problems. In the present analysis, the crack growth direction was chosen normal to the direction of maximum tensile stress. The general purpose finite element program ABAQUS (code version 6.9) was used (ABAQUS, 2002) with X-FEM. A three-dimensional finite element model has been developed to account for geometric and material behavior of SCB material plate. The finite element meshes constructed with hexagonal structural mesh, C3D8R (8-node linear brick) elements, are used under Standard/static analysis. The thickness of the plate is divided into 10 planar layers. Within each layer, the size of element decreases gradually with distance from the notch root decreasing. This means that the Finite Element (FE) meshes in the neighborhood of the notch root are much denser. The ratio of the small size element to the notch root is kept constant equals 0.1. The ABAQUS code was used for numerical calculation of $K_I$ and $K_{II}$ for the SCB specimen in each crack growth length a.

## RESULTS AND DISCUSSION

**Probable site of crack initiation:** To predict the site of crack initiation, the angular distribution of the normalized maximum tensile stress ($\sigma_{11}/\sigma_{ap}$) on the rim of the notch surface for different inclination angle, $\beta$, has been plotted in Fig. 2. The angular position ($\theta$) at the peak value of $\sigma_{11}/\sigma_{ap}$ is affected by $\beta$ and increased by increasing the value of $\beta$. The site of the peak value of $\sigma_{11}/\sigma_{ap}$ (site of crack intonation) was found at the point of the longest vertical coordinate on the notch rim for different inclination notch angle. Furthermore, the magnitude of the peak value of $\sigma_{11}/\sigma_{ap}$ decreased by increasing the value of $\beta$ for the same applied stress.

Figure 3 shows the site of crack initiation from notch root at different notch inclination angle, $\beta$ based on X-FEM. As shown in Fig. 3, the site of crack initiation was found as predicted in Fig. 2 at the point of the longest vertical coordinate on the notch surface for different inclination notch angle.

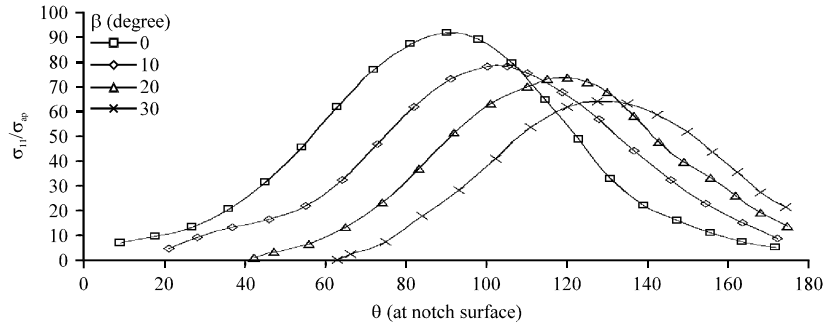


Fig. 2: Angular variation of normalized $\sigma_{11}/\sigma_{ap}$ on the rim of notch

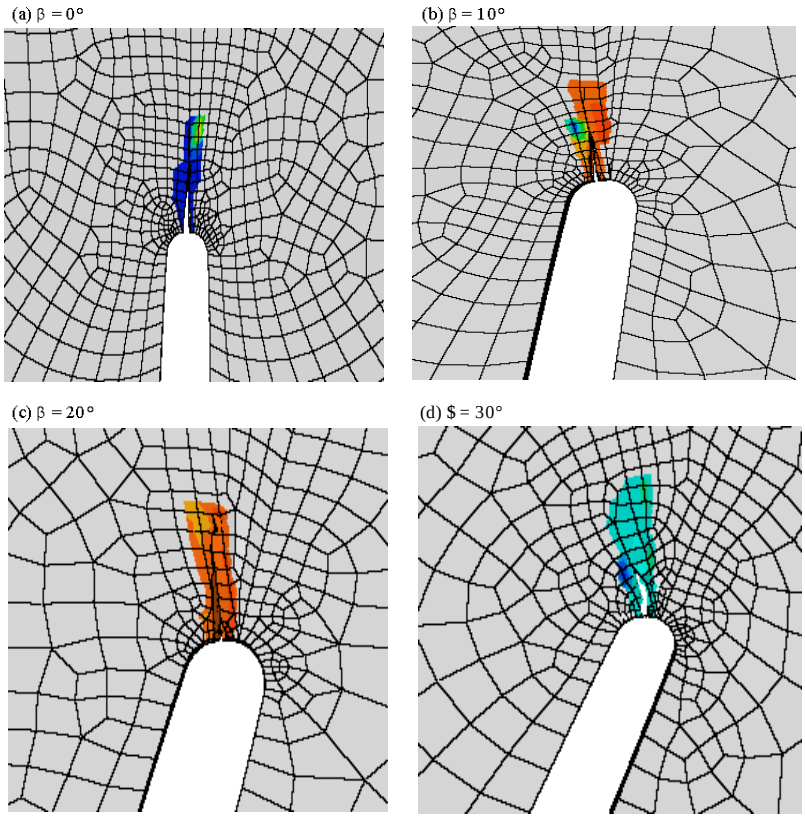


Fig. 3(a-d): The site of crack initiation from notch angle; (a) $\beta = 0°$, (b) $\beta = 10°$, (c) $\beta = 20°$ and (d) $\beta = 30°$

**Development of crack front shape:** Figure 4-7 show the development of the crack front shape through the depth of the plate for $\beta = 0$, 10, 20 and 30°, respectively, without using adaptive re-meshing technique. Examination of the figures reveals that for through-thickness SCB specimen, the crack exists at the mid-thickness of the specimen, i.e., $z = 0$. The sequence of the crack front formation showed that the extent of crack to spread out along the thickness direction was faster than the extension in the forward direction. This behavior is in agreement with that reported

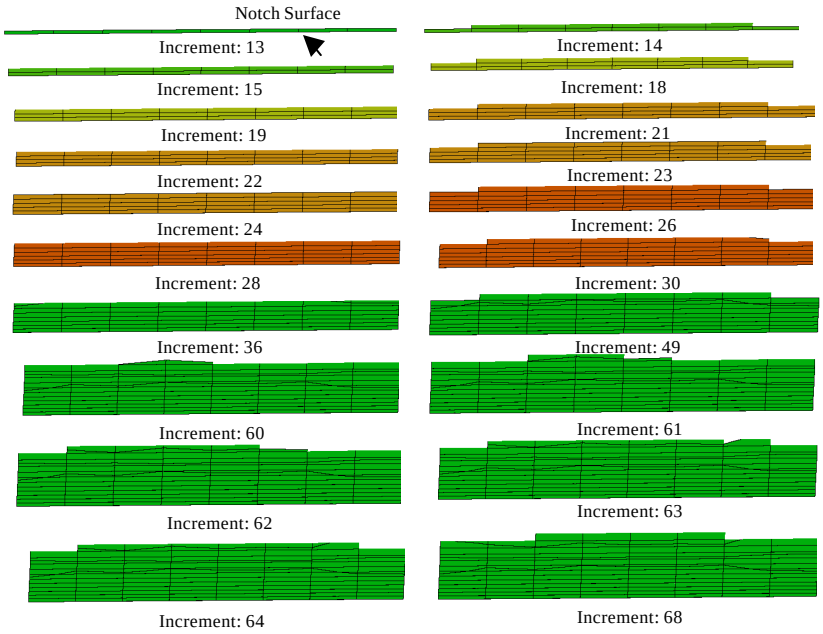


Fig. 4: Crack front development in SCB specimen by using XFEM for β = 0°

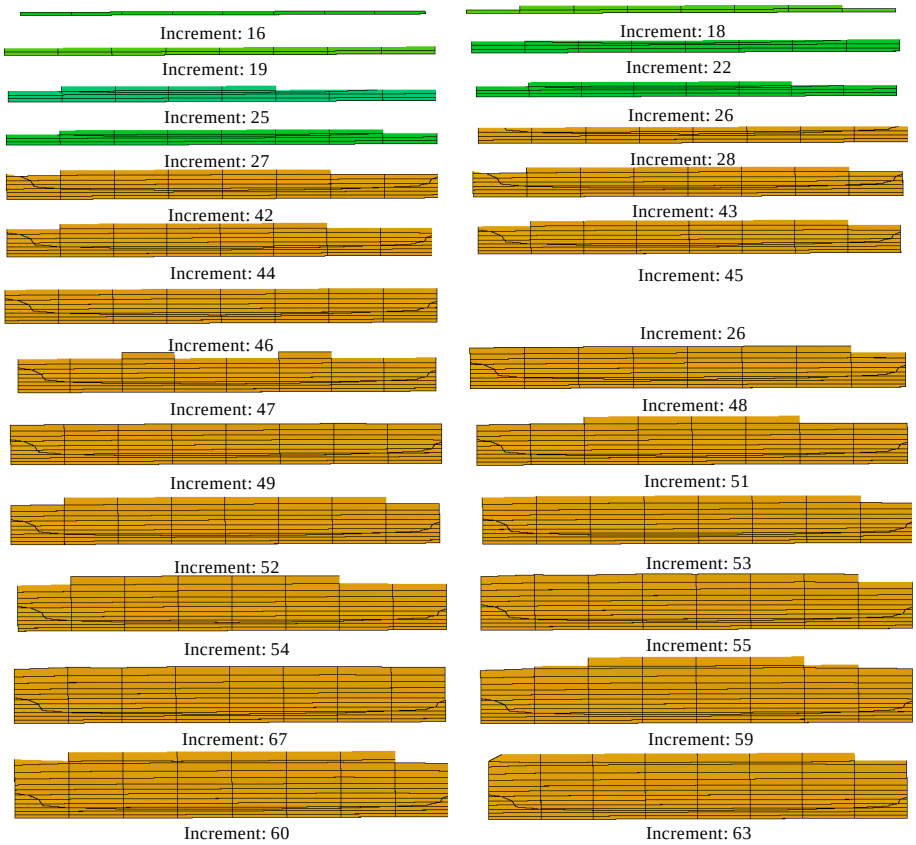


Fig. 5: Crack front development in SCB specimen by using XFEM for β = 10°

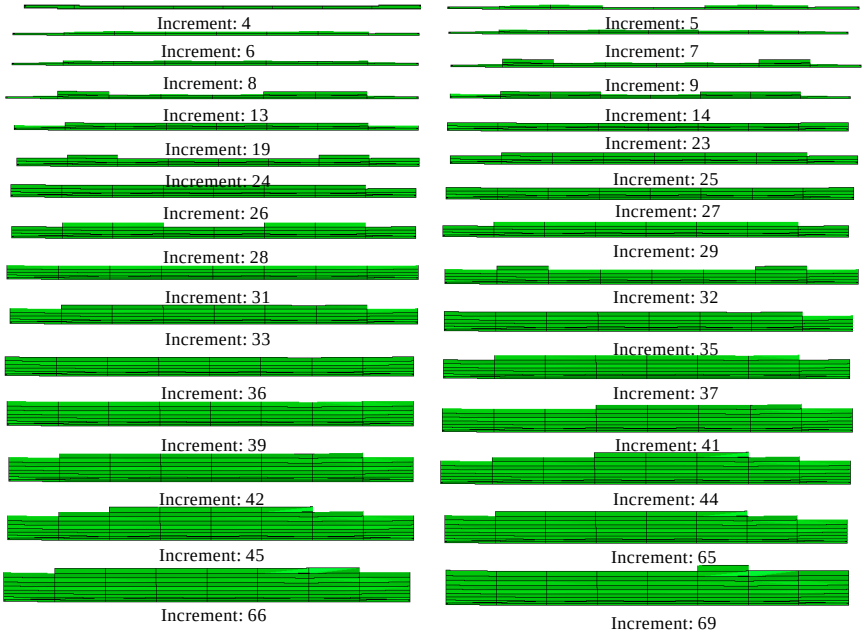


Fig. 6: Crack front development in SCB specimen by using XFEM for $\beta = 20^{o}$

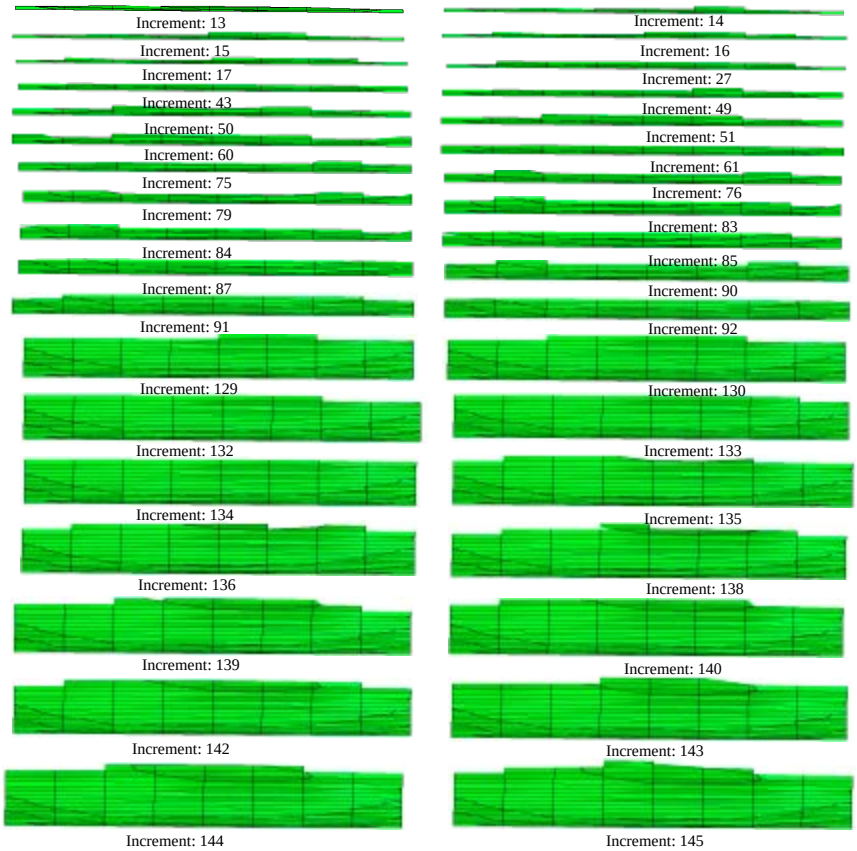


Fig. 7: Crack front development in SCB specimen by using XFEM for $\beta = 30^{o}$

by Hammouda *et al.* (1997) for crack front formation under pure mode I. Just the crack reaches the specimen surface, more growth was recorded in the forward direction. The crack grew in a self similar manner through the specimen thickness. In the case of mixed mode crack growth, some deviations were recorded but sill the shape of crack front is more or less as the thumb-nail shape. Recently, Sevcik *et al.* (2011) studied the effect of Poisson's ratio and specimen on the shape of crack front in two different specimen geometries (Middle Tension and 4-point bending) under pure mode I based on the assumption of a constant stress singularity exponent along the crack front. On the other hand, Liu *et al.* (2011) recently modified zigzag approach to predict the shape of crack front based on virtual crack closure-integral technique. The main advantage of their method is to avoid adaptive re-meshing technique.

**Crack path:** Figure 8 shows typical crack path in SCB specimen for crack emanating from notch with deferent **β**. An intuitive in the case of notch with zero inclination angle, the crack propagated perpendicular to the tensile stress. By increasing **β** (increasing mode II) fracture path deviates from the original inclination angle and grows along a curvilinear trajectory to extend toward the upper loading point. The present numerical results of crack path in SCB specimen for all **β** were in agreement with previous work of Aliha *et al.* (2010). So that XFEM is a good candidate to predict the crack path.

**Stress intensity factor:** The results of normalized stress intensity factor (Y) for mode I and mode II in the mid plan at z = 0 ($Y_{Imp}$ and $Y_{IImp}$, respectively) are tabulated in Table 1 for different notch inclination angle (**β**) and the length of the crack emanating from the notch (a).

Figure 9 shows the variation of The normalized $Y_I$ (the value of $Y_I$ is normalized by corresponding value of mid plane at z = 0) through the crack front of SCB specimen for different **β** (0°, 10°, 20° and 30°) and different crack length a. The normalized $Y_I$ increases with increasing the crack length, a. The maximum value of $Y_I$ shifted from the mid plane (z = 0) to the free surface with increasing the mode of crack mixity I/II, i.e., **β** increased. For **β** = 0°, the value of $Y_I/Y_{Imp}$

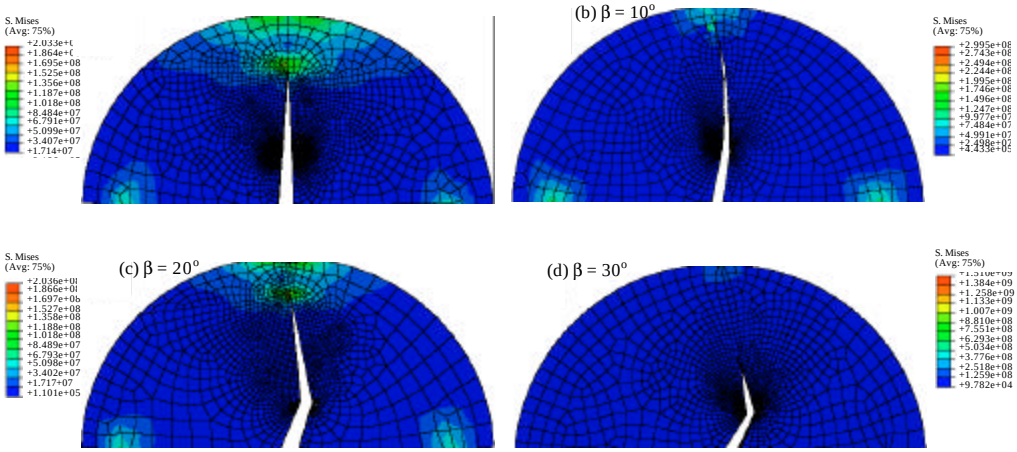


Fig. 8(a-d): Crack path in the SCB specimen for different inclination angle **β**

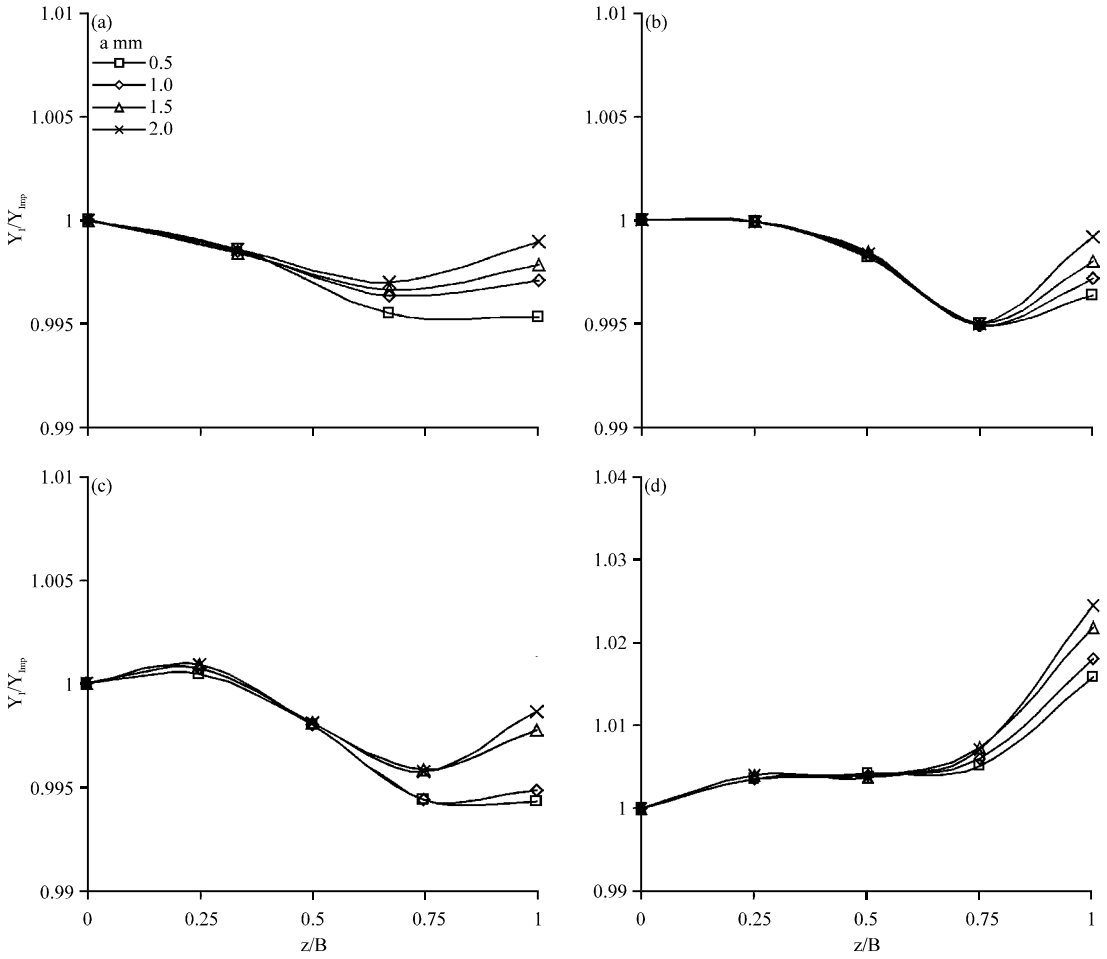


Fig. 9(a-d): Variation of normalized mode I stress intensity factor $Y_I$ through the crack depth for (a) $\beta = 0°$, (b) $\beta = 10°$, (c) $\beta = 20°$ and (d) $\beta = 30°$

Table 1: Normalized mode I and mode II stress intensity factor $Y_{Imp}$ and $Y_{IImp}$ at mid plane (at z = 0), for the SCB specimen

| | a (mm) | | | | |
|---|---|---|---|---|---|
| | β (degree) | 0.5 | 1 | 1.5 | 2 |
| $Y_{Imp}$ | 0 | 2.5294 | 2.5356 | 2.5624 | 2.5835 |
| | 10 | 2.4630 | 2.4854 | 2.5237 | 2.5440 |
| | 20 | 1.5271 | 1.8826 | 2.2970 | 2.3441 |
| | 30 | 1.3255 | 1.4750 | 2.1828 | 2.2152 |
| $Y_{IImp}$ | 0 | 0.0000 | 0.0000 | 0.0000 | 0.0000 |
| | 10 | 0.1101 | 0.1245 | 0.1451 | 0.1519 |
| | 20 | 0.1913 | 0.2518 | 0.3049 | 0.3110 |
| | 30 | 0.3425 | 0.3682 | 0.3849 | 0.4045 |

decreases with increasing z/B to reach a minimum value and then increasing to the free surface of plate. However, For $\beta = 10°$ and = 20°, the value of $Y_I/Y_{Imp}$ increases with increasing z/B to reach a maximum value then decreased to reach a minimum value and then increased again to the free

surface. Furthermore at $\beta = 30°$, $Y_I/Y_{Imp}$ increases with increasing z/B to reach the peak value at the free surface of the specimen. It can be concluded that, the maximum $Y_I$ do not always occur on the mid plane of the specimen and it occurs only on the mid plane in the case of pure mode I. The location of maximum $Y_I$ moves away from the mid plane of the specimen by increasing mode mixity I/II. On the other hand, near the mid plane of the specimen the value of $Y_I/Y_{Imp}$ is independent on the crack length, while, this value is highly affected by the crack length at the specimen surface and increased by increasing the crack length for all values of mode of mixity.

Figure 10 shows the influence of $\beta$ on the normalized $Y_{II}$ (the value of $Y_{II}$ is normalized by the corresponding value at the mid plane) through the crack front for different $a$. The normalized value of $Y_{II}$ increased by increasing the value of z/B to reach the maximum value at the free surface of specimen for all values of mode mixity. It can be observed an opposite trend to $Y_I/Y_{Imp}$ which the value of $Y_{II}/Y_{IImp}$ at the specimen surface decreased by increasing of crack length.

Figure 11 shows the variation of the normalized mode I stress intensity factor ($Y_I$) at the specimen surface with $\beta$ for different crack length, a. It can be concluded that, the effect of the crack length on $Y_I$ at the surface is more pronounced in a higher value of mode of mixity.

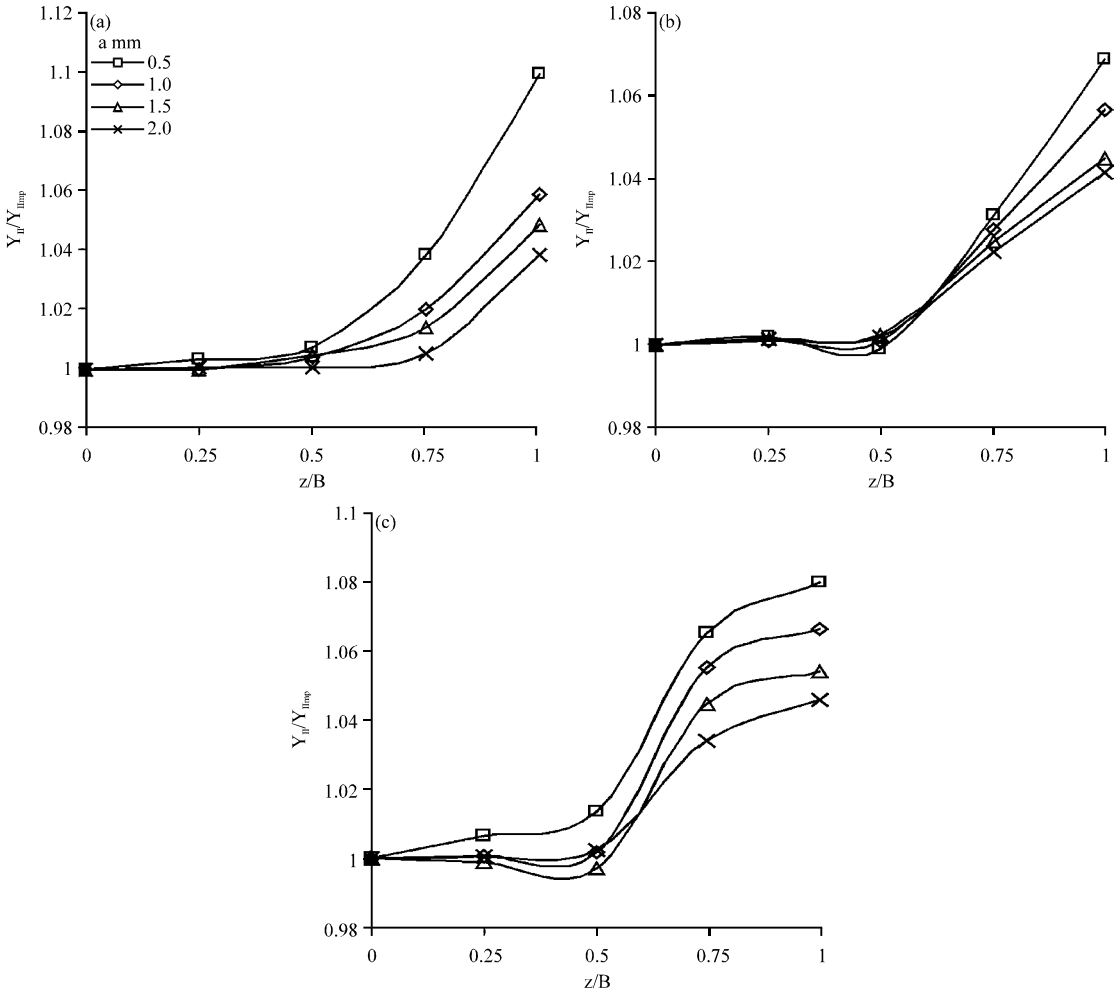


Fig. 10(a-c): Variation of normalized mode II stress intensity factor $Y_{II}$ through the crack depth for (a) $\beta = 10°$, (b) $\beta = 20°$ and (c) $\beta = 30°$

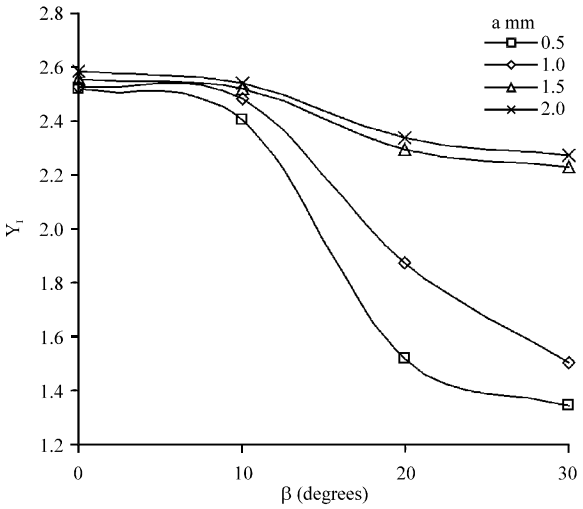


Fig. 11: Variation of normalized mode I stress intensity factor $Y_I$ with **β**

## CONCLUSIONS

Based on the present numerical results the following conclusions were drawn:

- The site of crack initiation in notched SCB specimen was found as at the point of the longest vertical coordinate on the notch surface for different inclination notch angle
- The develop of crack front shape is little effect by the value of mode of mixity and the shape of crack front is still more or less as the thumb-nail shape
- Extend finite element method is a good candidate to predict the crack path in SCB specimen under different mode mixity
- the maximum value of $Y_I$ occurs only on the mid plane in the case of pure mode I. Furthermore, its location moves away from the mid plane to the surface of the specimen by increasing the value of the mode mixity
- $Y_I$ at the specimen surface increased by increasing the crack length for all values of mode of mixity, while, the opposite trend was found in the case of $Y_{II}$

## REFERENCES

ABAQUS, 2002. User's Manual Version 6.3. Hibbitt, Karlsson and Sorensen Inc., Pawtucket, RI., USA.

Aliha, M.R.M., M.R. Ayatollahi, D.J. Smith and M.J. Pavier, 2010. Geometry and size effects on fracture trajectory in a limestone rock under mixed mode loading. Eng. Fract. Mech., 77: 2200-2212.

Ayatollahi, M.R. M.R.M. Aliha and M.M. Hassani, 2006. Mixed mode brittle fracture in PMMA-An experimental study using SCB specimens. Mat. Sci. Eng. A., 417: 348-356.

Ayatollahi, M.R. and M.R.M. Aliha, 2008. On the use of Brazilian disc specimen for calculating mixed mode I-II fracture toughness of rock materials. Eng. Fract. Mech., 75: 4631-4641.

Ayatollahi, M.R.M. and M.R. Aliha, 2007. Wide range data for crack tip parameters in two disc-type specimens under mixed mode loading. Comput. Mater. Sci., 38: 660-670.

Beng, Y.K., M.N. Dalimin and M.A. Faizal, 2007. Mode-I toughness and curing pressure characteristic of symmetrical lay-up of plain-weave woven GFRP composites. J. Applied Sci., 7: 2174-2182.

Hammouda M.M.I., M.H. Seleem, H.E.M. Sallam and S.S.E. Ahmad, 1997. Simulation of closure during front development of a fatigue crack. Proccdings of th 6th International Confernce on Production Engeenering Design and Control, February 15-17, 1997, Alexandria, Egypt.

Hammouda, M.M.I., A.S. Fayed and H.E.M. Sallam, 2004. Stress intensity factors of a central slant crack with frictional surfaces in plates with biaxially loading. Int. J. Fracture, 129: 141-148.

Liu, Y.P., C.Y. Chen and G.Q. Li, 2011. Modified zigzag approach to approximate moving crack front with arbitrary shape. Eng. Fract. Mech., 78: 234-251.

Muthurajan, K.G., K. Sankaranarayanasamy, S.B. Tiwari and B. Nageswara Rao, 2006. Evaluation of carbon/epoxy delamination fracture toughness. Trends Applied Sci. Res., 1: 144-154.

Ouinas, D., A. Hebbar and J.V. Olay, 2006. Fracture mechanics modelling of cracked aluminium panel repaired with bonded composite circular patch. J. Applied Sci., 6: 2088-2095.

Ravichandaran, R. and G. Thanigaiyarasu, 2011. Mixed-Mode fracture analysis of aluminum alloy 5083 subjected to four point bending. J. Applied Sci., 11: 2214-2219.

Sevcik, M., P. Hutar, M. Zouhar and L. Nahlik, 2011. Numerical estimation of the fatigue crack front shape for a specimen with finite thickness. Int. J. Fatigue, (In Press).

Shah, Q.H., H. Homma, M.H. Iliyas and A.F. Ismail, 2005a. The effect of material property gradient on the fracture toughness of a PMMA/PC bimaterial with a crack normal to the interface. J. Applied Sci., 5: 476-481.

Shah, Q.H., M. Azram and M.H. Iliyas, 2005b. Predicting the crack initiation fracture toughness for a crack along the bimaterial interface. J. Applied Sci., 5: 253-256.

Shariati, M. and M.J. Maghrebi, 2009. Experimental study of crack growth behavior and fatigue life of spot weld tensile-shear specimens. J. Applied Sci., 9: 438-448.

Zenasni, R., A. Hebbar and J. Vina olay, 2006. Time storage effect of the resin on the toughness of a unidirectional carbon fibre. J. Applied Sci., 6: 2641-2646.

Zulkifli, R., K.S. Pei and C.H. Azhari, 2008. Interlaminar fracture properties of multi-layer woven silk fibre/polyester composites. Asian J. Applied Sci., 1: 177-184.